

Dramatic performance enhancement of evanescent-wave multimode fiber fluorometer using non-Lambertian light diffuser

Jianjun Ma and Wojtek J. Bock

*Centre de recherche en photonique, Département d'informatique et d'ingénierie,
Université du Québec en Outaouais,
P.O. Box 1250, Station B, Gatineau, Québec J8X 3X7, Canada,
ma.jianjun@uqo.ca, wojtek.bock@uqo.ca*

Abstract: To enhance the performance of an evanescent-wave (EW) based sensor, efforts are usually made to modify the sensor architecture rather than the excitation source. In this paper, we theoretically examine the role of meridian and skew rays under total internal reflection (TIR) as well as tunneling rays with the emphasis on sensor performance. Our further investigation indicates that the intensity profile of the light source enormously influences the EW power, and thus the collectable fluorescent emission level as well. A non-Lambertian fiber-optic side-emitting diffuser (FOSED) is proposed and experimentally verified, revealing that a proper alignment of this FOSED can dramatically improve the signal quality and reduce the level of stray excitation light. In particular, the adoption of a FOSED or other light diffusers with similar output profiles will ensure that the excitation power is used more efficiently, suggesting a lower demand on the excitation source power level, and the performance of the stray light filter and detector. The superiority of this innovation is further addressed by comparing it with a long period grating (LPG) fiber-optic sensor, which claims highly efficient core to cladding mode coupling. This study presents a new concept for the construction of a high-performance and cost-effective EW-based sensor system.

©2007 Optical Society of America

OCIS codes: 300.6280 Spectroscopy, fluorescence and luminescence; 230.1980 Diffusers; 230.6080 Sources; 060.2340 Fiber optics components; 060.2370 Fiber optics sensors; 060.2380 Fiber optics sources and detectors.

References and Links

1. J. Enderlein, T. Ruckstuhl, and S. Stefean, "Highly efficient optical detection of surface-generated fluorescence," *Appl. Opt.* **38**, 724-732 (1999).
2. L. Polerecky, J. Hamrle, and B. D. MacCraith, "Theory of the radiation of dipoles placed within a multilayer system," *Appl. Opt.* **39**, 3968-3977 (2000).
3. D. Marcuse, "Launching light into fiber cores from sources located in the cladding," *IEEE J. Lightwave Technol.* **6**, 1273-1279 (1988).
4. E. H. Lee, R. E. Benner, J. B. Fenn, and R. K. Change, "Angular distribution of fluorescence from liquids and monodispersed spheres by evanescent wave excitation," *Appl. Opt.* **18**, 862-868 (1979).
5. C. R. Taitt, G. P. Anderson, and F. S. Ligler, "Evanescent wave fluorescence biosensors," *Biosens. Bioelectron.* **20**, 2470-2487 (2005).
6. L. C. Shriver-Lake, K. A. Breslin, P. T. Charles, D. W. Conrad, J. P. Golden, and F. S. Ligler, "Detection of TNT in water using an evanescent wave fiber-optic biosensor," *Anal. Chem.* **67**, 2431-2435 (1995).
7. R. M. Wadkins, J. P. Golden, L. M. Pritsiolas, and F. S. Ligler, "Detection of multiple toxic agents using a planar array immunosensor," *Biosens. Bioelectron.* **13**, 407-415 (1998).
8. S. Ekgasit, C. Thammacharoen, F. Yu, and W. Knoll, "Evanescent field in surface plasmon resonance and surface plasmon field-enhanced fluorescence spectroscopies," *Anal. Chem.* **76**, 2210-2219 (2004).
9. N. Fang, Z. Liu, T.-J. Yen, and X. Zhang, "Experimental study of transmission enhancement of evanescent waves through silver films assisted by surface plasmon excitation," *Appl. Phys. A* **80**, 1315-1325 (2005).

10. R. C. Jorgenson and S. S. Yee, "A fiber-optic chemical sensor based on surface plasmon resonance," *Sens. Act. B*, **12**, 213-220 (1993).
11. R. Slavik, J. Homola, J. Ctyroky, and E. Brynda, "Novel spectral fiber optic sensor based on surface plasmon resonance," *Sens. Act. B*, **74**, 106-111 (2001).
12. N. Calander and M. Willander, "Optical field enhancement by surface-plasmon resonance: Theory and application to micro-bioelectronics," in *Proceedings of IEEE conference on Optoelectronic and Microelectronic Materials and Devices* (IEEE 2002), 531-536 (2002).
13. T. Ruckstuhl and D. Verdes, "Supercritical angle fluorescence (SAF) microscopy," *Opt. Express* **12**, 4246-4254 (2004)
<http://www.opticsinfobase.org/abstract.cfm?URI=oe-12-18-4246>
14. R. Blue, N. Kent, L. Polerecky, H. McEvoy, D. Gray, and B.D. MacCraith, "Platform for enhanced detection efficiency in luminescence-based sensors," *Electron. Lett.* **41**, 682-684 (2005).
15. J. -F. Gouin, A. Goyle, and B. D. MacCraith, "Fluorescence capture by planar waveguide as platform for optical sensors," *Electron. Lett.* **34**, 1685-1686 (1998).
16. J. P. Golden, G. P. Anderson, S. Y. Rabbany, and F. S. Ligler, "An evanescent wave biosensor- Part II: Fluorescent signal acquisition from tapered fiber optic probes," *IEEE Trans. Biomed. Eng.* **41**, 585-591 (1994).
17. Y. Raichlin, L. Fel, and A. Katzir, "Evanescent-wave infrared spectroscopy with flattened fibers as sensing elements," *Opt. Lett.* **28**, 2297-2299 (2003).
18. See RAPTOR™ 4-channel bioassay system made by Research International, Inc., available at <http://www.resrchintl.com/raptor-detection-system.html>.
19. E. E. Carlyon, C. R. Lowe, D. Reid, and I. Bennion, "A single mode fiber-optic evanescent wave biosensor," *Biosens. Bioelectron.* **7**, 141-146 (1992).
20. Z. M. Hale, F. P. Payne, R. S. Marks, C. R. Lowe, and M. M. Levine, "The single mode tapered optical fiber loop immunosensor," *Biosens. Bioelectron.* **11**, 137-148 (1996).
21. T. R. Glass, S. Lackie, and T. Hirschfeld, "Effect of numerical aperture on signal level in cylindrical waveguide evanescent fluorosensors," *Appl. Opt.* **26**, 2181-2187 (1987).
22. J. Ma and W. Bock, "Reshaping sample fluid droplet: toward combined performance enhancement of evanescent-wave fiber-optic fluorometer," *Opt. Lett.* **32**, 8-10 (2007).
23. D. Gloge, "Weakly guiding fibers," *Appl. Opt.* **10**, 2252-2258 (1971).
24. A. W. Snyder and J. D. Love, *Optical Waveguide Theory* (Chapman and Hall, 1983).
25. G. Keiser, *Optical fiber communications* (McGraw-Hill Higher Education, third edition, 2000), Ch. 5.
26. M. J. Adams, D. N. Payne, and F. M. E. Sladen, "Leaky rays on optical fibers of arbitrary (circularly symmetric) index profiles", *Electron. Lett.* **11**, 238-240 (1975).

1. Introduction

In chemical, biological and clinical sample studies, devices based on evanescent-wave (EW) technology are typically preferred tools for optical sensing. This preference is dictated by several specific challenges commonly encountered in these research areas. First, liquid samples containing concentrations of several species are often involved. Second, fluorescent or Raman spectrum is the chosen signal type for sample assay because it reflects the attributes of these species. Unfortunately, such signals have very low power levels. Third, although these low-level signals can be enhanced by increasing the excitation power, side effects such as photo bleaching may occur to the species and will prevent the excitation level from rising much. Fourth, during the period of sample assay, a variety of complex events may occur simultaneously, including chemical reactions, change of excitation / emission or scattering light absorption stemming from it as well as noise from stray ambient light. These events pose severe challenges to signal recovery for many existing optical means.

Instead of dealing with all these challenges, EW technology offers a solution by choosing a local sample volume subject to minimal outside influence. In contrast to the procedure used in many other optical means, excitation light is not directly launched into the sample volume. Rather, it is first reshaped to allow only limited power to penetrate into the sample side for an extremely short distance. This power is carried by an EW formed via total internal reflection (TIR) in the contact surface between the sample and the optical device. The fact that most liquid samples have a lower refractive index (RI) than optical glass guarantees the occurrence of TIR hence the formation of EWs. The penetration depth of EWs ranges from several hundred nanometers to approximately one wavelength above the contact surface. Three important features of EW technology are:

1. this thin layer of penetration means there is a short light-path to the optical device. Both excitation power delivery and signal collection will be highly efficient because they experience minimum attenuations;

2. the sample layer is excited uniformly. The total signal light collected is the sum of signals from all excited sites. Local photo bleaching due to the focused power can thus be avoided; and

3. signal detection at the optical device side is not a straightforward process. Instead, for a device with one or multiple planar surfaces, one of the models, electric dipole, explains the responsible mechanism, showing that only the dipoles in this EW layer have the highest coupling efficiency [1, 2]. Coupling from any dipoles beyond this layer drops dramatically, suggesting that the ambient light from any processes above the EW layer will be efficiently blocked in a natural way. A fiber-optic version of interpretation is also presented via wave-optics theory [3], again showing a much higher signal level from this EW layer. Consequently, an EW-based device is an excellent tool for surface event analysis, offering an extremely high signal-to-noise ratio and an outstanding solution to those challenges highlighted at the beginning of this section.

Here, based on wave-optics, we provide a more intuitive interpretation of how the fluorescent light is coupled back to the fiber core and becomes guided, which is considered to be an impossible process from the ray-optics point of view. Mode theory suggests that a guiding mode capable of collecting light from the lower RI medium side must have its mode field extended into the cladding region, or sample area in our discussion. This extended portion of mode field is called EW tail, which overlaps with the fluorescent light field launched from the sample. The coupling of the fluorescent light power to this guiding mode thus occurs via this tail. The percentage of this tail field over the entire mode field is critical. A larger percentage of the mode field in the cladding side, associated with a higher-order guiding or a tunneling mode, means better collection capability. However, the mode is more vulnerable to the interferences from outside of the core. A shorter EW tail, corresponding to a lower-order guiding mode, guarantees better confinement and less attenuation over a long distance but suffers poorer collection capability. All valid guiding modes will have their EW tails falling into a thin layer, which is called EW layer as described before. Such a concept clearly explains why almost all collected signal is carried by the higher-order guiding mode group or the ray group traveling around the critical angle, as indicated by others from their detailed theoretical calculations [1, 2].

Various forms of EW-based devices have been developed. Examples include those based on free-space optics [4], fiber-optics [5, 6] and the lab-on-a-chip concept [7]. These three categories are widely reported in the research literature, and some devices incorporating these technologies are commercially available. However, there are two commonly encountered problems: the weak level of EW power and the strong stray excitation light. The availability of high-performance filters has made the second problem less important. Many efforts have thus focused on how to enhance the sensor sensitivity via modification of EWs in various ways. One well-known example is the use of surface plasmon resonance (SPR) to improve sensor performance through attenuated total internal reflection (ATIR) with the assistance of either a precious metal layer whose thickness is strictly controlled or a group of nano-sized metal particles. SPR-based technology has been explored for a variety of devices including free-space based devices [8, 9], fiber-optic devices [10, 11] and lab-on-a-chip devices [12]. With SPR, the EW of the *p*-polarized light incident at the metal / dielectric interface interacts with surface plasmons (oscillating electrons) under a resonant condition. Energy transfer from the EW to the plasmons thus occurs. The associated reflected light is hence strongly attenuated, implying that its energy is depleted by transfer to the plasmons over the EW. As a result, the overall sensitivity of the sensor is greatly enhanced. Measurement is performed by examining the missing energy. In other words, properties of the sample can be found by measuring the power drop in the signal, either by angle-scanning the reflected monochromatic light or by examining the notch appearing in the spectrum of a broad-band light source after reflection.

Using SPR is certainly a somewhat indirect way to improve the performance of an EW-based system. An alternative and more straightforward approach is to directly enhance the EW power level and / or the signal collection efficiency. One proposal has been demonstrated for a free-space based apparatus consisting of a parabolic reflector specifically designed to enhance signal collection. Underlying this approach is the fact that maximum emission occurs at the critical angle and its vicinity [1, 13]. Similarly, a lab-on-a-chip version of such a device has also been investigated [14, 15], possessing the potential of low-cost mass production. In the area of fiber-optic EW sensor research, a particular focus of interest is the taper. For several decades, tapers formed at the tip or middle portion of the fiber have attracted serious attention as a means of boosting the EW level, which arises from the increased numerical aperture (NA) in the tapered region, allowing EWs to penetrate deeper into the sample. Moreover, the collectable emission signal is naturally coupled to the lower-order guiding modes, dramatically reducing the signal loss and increasing signal stability during transmission [16-18]. Single-mode fibers (SMFs) or few-mode fibers with side-polished cores have also been exploited [19, 20], taking advantage of the large portion of core mode field traveling in the cladding in the form of EWs. Furthermore, the combination of SMFs with tapering [20] and SPR [11] has been explored.

Reduction of stray excitation light strength has also been targeted in the research. Reflection-type fiber-optic EW sensors were thought to be better in this regard than their transmission-type counterparts [21] and proof of this has been seen in the research. Other non-fiber-optic designs [14-16] can possibly eliminate the stray excitation background. We have recently demonstrated that a fiber-optic version of the EW sensor [22] can simultaneously enhance the EW level and completely remove background noise without a filter.

Amongst the many research proposals for EW power enhancement and background suppression so far, no effort has been made to modify the light source itself. In fact, in a typical EW-based device, be it a free-space apparatus or a fiber-optic or a lab-on-a-chip version, most of the excitation power makes no contribution to enhancing the EW power. Instead, the major portion of the excitation power becomes a strong background usually much stronger than the emission signal. In this paper, based on a transmission-type fiber-optic EW sensor, well-known for its strong background as indicated before, we will demonstrate, both theoretically and experimentally, that a non-Lambertian type diffuse light source can significantly improve the signal quality. As we shall see in our later discussion, such a modification offers a cost-effective route to performance enhancement of EW-based devices.

2. Theoretical background

2.1 Re-examining the mode groups harmful to a fiber-optic communication system: their positive effects on an EW fiber-optic sensor system

Both higher-order guiding and tunneling modes are generally considered as two negative factors on dispersion of a fiber-optic communication system. They were intensively discussed in the first decade when the optical fiber appeared to be an excellent optical signal carrier. In particular, they proved to be harmful to the long-haul fiber-optic communication system. This is also the major reason why single-mode fibers become the major optical signal carriers later on in long haul fiber-optic communication systems although their tiny cores pose severe challenges on each optical element in the system, each service equipment and the overall system cost.

Higher-order guiding mode group is considered to be a major contributor for the performance of an EW fiber-optic sensor [5]. Although the general mode theory has indicated that like lower-order guiding modes, higher-order guiding modes can also be formed by both meridian rays and skew rays, no further discussions were made to prove how to fully use these characteristics to maximize the sensor performance. Further, another mode category, tunneling mode, is ignored in the fiber-optic sensor related discussions. As we shall see later, the tunneling mode group can play more important role in an EW fiber-optic sensor system.

This is due to two factors: first, the number of tunneling modes is close to the population of the overall guiding modes; second, the EW tail of a tunneling mode is cascaded with an oscillating field, which further extends into the cladding. The excitation of tunneling modes is expected to add more power to the sample area and leads to a further enhancement of the fluorescent signal collection efficiency. This is especially important when the fiber length involved is in the order of kilometers or less, which is often the case for fiber-optic sensors. This paper will address the characteristics of higher-order guiding modes and tunneling modes together and proposes a novel way to excite them simultaneously, which will maximize the EW sensor performance.

In many published papers and textbooks, meridian ray model, stemming from the slab waveguide concept, is often discussed in more detail due to its simplicity. Aforementioned skew rays associated with the two mode groups are usually discussed little. This may suggest to the readers that skew rays are not really important. Of course, associated but complex theoretical discussions regarding all these ray or mode groups are seen in professional journals or books. But an immediate and clear picture of what occurred to these ray or mode groups in a multimode fiber (MMF) without addressing complex formulae is also important. This is particularly the case to those who are working on specific fiber-optic sensor related applications but having their backgrounds in chemical, biological and medical sectors. In today's research, there are increasing demands on fiber-optic technology from these sectors for variety of sample assays. The tendency of research and products also indicates that the future of fiber-optic sensors may heavily rely on their demands. Moreover, large amount of evidences show that MMFs are dominating their research and even commercial products due to the unbeatable advantages of the MMFs. Putting all fragments of the most important characteristics of each ray or mode groups together to form a complete picture of MMF for these researchers would be indeed valuable. This paper intends to fill this niche by presenting all three ray groups (meridian and skew ray groups under TIR and tunneling ray group) together with the emphasis on skew rays under TIR and tunneling rays in a reader-friendly manner, which has not been done before. In association with them, the guiding and the tunneling modes are the terms often used when the concept needs the mode theory to interpret.

2.2 Classical interpretation of EW strength in the cladding via meridian rays

In many articles, the behavior of rays traveling in a slab waveguide is used to describe what occurs in a fiber core-cladding interface, and the effects of the curved wall of the fiber core are simply ignored since only meridian rays exist in slab waveguides. However, the description makes the analysis simple and clear in concept. Applying this concept to an EW sensor based on an MMF, the EW strength in the cladding side highly depends on the power carried by high-order guiding mode groups. The illustration of rays in the EW field in Fig. 1 indicates that higher-order guiding modes are described as steeper rays. Rays with an incident angle approaching the critical angle θ_c will extend into the cladding much further. Using subscripts "1" and "2" to represent the core and cladding, respectively, the EW field is expressed by:

$$E_2 = E_{20} \exp(-\gamma_2 \cdot |x|) \exp(-i\beta z), \quad (1)$$

which propagates only in the z direction and decreases in amplitude when $|x|$ increases. Here γ_2 is the attenuation coefficient of the guiding mode in the cladding side and β is the mode phase propagation constant. The coefficient γ_2 is:

$$\gamma_2 = n_2 k_0 \sqrt{\left(\frac{n_1}{n_2}\right)^2 \sin^2 \theta_1 - 1}, \quad (2)$$

where n_1 and n_2 are the RI of the core and cladding, respectively. θ_1 is the incident angle of a ray at the core-cladding interface for TIR formation and $k_0 = 2\pi / \lambda_0$ is the wave number in free space.

Clearly, from Eq. (2), a larger incident angle θ_1 leads to a tighter confinement of the wave within the fiber core, suggesting that the favorable level of emission power strongly connects with the group of excitation rays close to the critical angle.

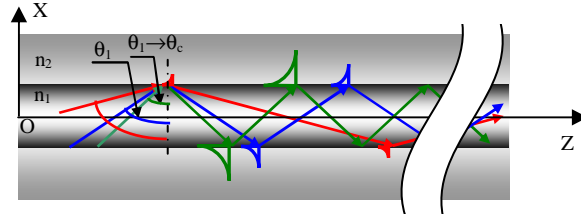


Fig. 1. Representation of rays in the EW field, indicating deeper penetration of EW field when ray incident angles approach the critical angle.

2.3 Estimate of the EW power carried by pure guiding modes far from cutoff based on mode theory

The simplified model presented above provides no clue for calculating the excitation power level in the cladding side. Mode theory is needed for such an estimate. For a step-indexed MMF with a large mode volume, Gloge [23] found that the power flow in the cladding approximately obeys the following formula:

$$\frac{P_{clad}}{P_{core} + P_{clad}} \approx \frac{1.33}{\sqrt{N}} \approx \frac{1.89}{V} \quad (3)$$

where P_{clad} and P_{core} represent the total power flow in the cladding and core regions, respectively. V is the normalized frequency expressed by:

$$V = \frac{2\pi}{\lambda} r \sqrt{n_1^2 - n_2^2} \quad (4)$$

where r is the fiber core radius, λ is the wavelength and N is the total number of guiding modes calculated by:

$$N = \frac{V^2}{2} \quad (5)$$

The prerequisite for Eq. (3) is that all modes must be excited equally and only the guiding modes far from cutoff are considered.

For a step-indexed MMF with a core size of 400 μm , a core / cladding refractive index of 1.46 / 1.41 and an Argon laser wavelength of 488 nm, from Eq.(3) ~ Eq.(5) we find:

$$\frac{P_{clad}}{P_{core} + P_{clad}} \approx 0.2\% . \quad (6)$$

This is a quite small figure. However, even such a small amount of power is difficult to achieve since almost all light sources have non-uniform intensity profiles. A typical profile is Gaussian-like, and is found in LEDs and halogen white lamps as well as lasers. The usual way of coupling from these sources leads to most of the power being carried by lower-order guiding mode groups. While this is generally advantageous for fiber-optic communication system, in an EW-based fiber-optic sensor system, it becomes a source of strong noise and results in a much weaker signal.

2.4 Tunneling modes: An unusual mode group for dramatic enhancement of EW sensor signal level

According to Snyder et al. [24, Ch. 7], in a fiber waveguide, rays may fall into either of two classes: bound rays and refracting rays. Bound rays, corresponding to guiding modes, travel along the waveguide via TIR. Refracting rays, associated with leaky modes, will radiate their energy and completely disappear within an extremely short distance. Refracting rays generally do not affect system performance. However, the fiber waveguide allows a third class of rays to exist. These are distinct from both bound and refracted rays, and are called tunnelling rays. In terms of wave-optics, tunnelling rays with the same incident angles form one ray congruence in association with one mode known as a tunnelling mode. An important feature of the tunnelling mode is that it possesses extremely low attenuation even over a long-distance transmission, which can be kilometers in length. Unlike guiding modes, which are derived from the real β solutions of the eigenvalue equation with β as the propagation constant or eigenvalue of the mode, tunnelling modes are found from certain complex β solutions of the eigenvalue equation and are associated with the mode groups operating just below cutoff. Therefore, the most critical difference between the two modes is that the modal parameters of tunnelling modes appearing in the fields are complex, leading to radiation of the energy. In terms of ray optics, tunnelling rays, like leaky rays, undergo partial reflection [10]. However, they do not experience refraction. Instead, their attenuation is exclusively due to the curvature of the fiber cross-section. These rays tunnel from the core-cladding boundary through the evanescent region adjacent to the core and emerge some distance from the boundary and lose their power which is called a radiation caustic. In direct contrast to what occurs with slab waveguides, a significant portion of the radiation field can persist for enormous distances within the circular MMF waveguide with $V \gg 1$. All tunnelling rays must be skewed to the fiber axis to fulfill the above unusual characteristics. Furthermore, unlike a higher-order guiding mode with only an EW field residing in the EW layer, a tunnelling mode has an EW tail cascaded with an additional oscillating wave field that extends even further into the cladding. This characteristic endows tunnelling modes with a greater capacity than higher-order guiding modes to contribute excitation power and receive fluorescent signal tunneled back from the sample. This is particularly significant for an EW fiber-optic sensor, where the fiber length can typically be measured in meters.

There are more tunnelling modes than guiding modes in a step-indexed MMF. The number can be calculated by the following equation [24, Ch. 36]:

$$\frac{N_{ml}}{N_g} \approx 1 + \frac{(2\Delta)^{1/2}}{3\pi}, \quad (7)$$

where N_{ml} represents the number of tunnelling modes, assuming $\Delta \ll 1$. For a weakly guided MMF, the number of tunnelling modes is roughly the same as the number of guiding modes.

2.5 Maximum light acceptance angle of meridian, skew and tunneling rays

In the field of ray optics, the light acceptance angle is often referred to in terms of the NA corresponding to meridian rays under TIR [25]:

$$NA_{mdn} = n_0 \sin \theta_{0mdn} = \sqrt{n_1^2 - n_2^2} \quad (8)$$

where θ_{0mdn} is the maximum half-angle of the acceptance cone of the meridian rays and n_0 is the refractive index of the medium outside the fiber core end face. When the medium is air, $n_0 = 1$.

The guiding mode group is also associated with a large number of skew rays which are under TIR. Although tunnelling rays are often referred to as skewed, they are in fact leaky rays. As indicated in Fig. 2(a), under TIR, skew rays exist and travel off the core center O.

Their trajectories projected onto the end face of the fiber core form a closed loop near the core-cladding interface. Skew rays never cross the fiber axis and can be launched from anywhere \mathbf{r} across the core surface. One such ray, lying in the plane ACGE, has an angle γ with the meridian plane ADHE, where meridian rays are found. From the geometry of Fig. 2(a), the following relationship exists under the assumption of TIR:

$$\cos \gamma \cdot \sin \theta_t = \cos \phi = \sqrt{1 - \frac{n_2^2}{n_1^2}} \quad (9)$$

The general requirement governing the incident angle θ_{skw} of skew rays can hence be simply derived from Snell's law:

$$n_0 \sin \theta_{skw} \geq \frac{\sqrt{n_1^2 - n_2^2}}{\cos \gamma} = \frac{NA_{mdn}}{\cos \gamma} \geq NA_{mdn} \quad 0 < \gamma < \frac{\pi}{2} \quad (10)$$

From this it is clear that the NA of meridian rays is only the special case of Eq. (10) when $\gamma = 0$. Clearly, $\theta_{skw} \geq \theta_{0mdn}$, suggesting that the minimum incident angle of skew rays starts from the maximum acceptance angle of meridian rays. In other words, the guiding modes associated with skew rays can be excited only by rays outside the maximum acceptance cone of meridian rays, including rays with incident angles close to $\pi/2$. Furthermore, as in Fig. 2(a), each meridian plane is associated with many skew planes since γ can vary over a wide range of values. In this regard, there are far more skew than meridian rays in an MMF waveguide. In particular, this also implies that in contrast to meridian rays, there are far more skew rays with steeper incident angles. They are associated with the mode group having a higher proportion of the EW field extending into the cladding and thus their effects on sensor performance are far more important, especially when a fiber with large mode volume is involved.

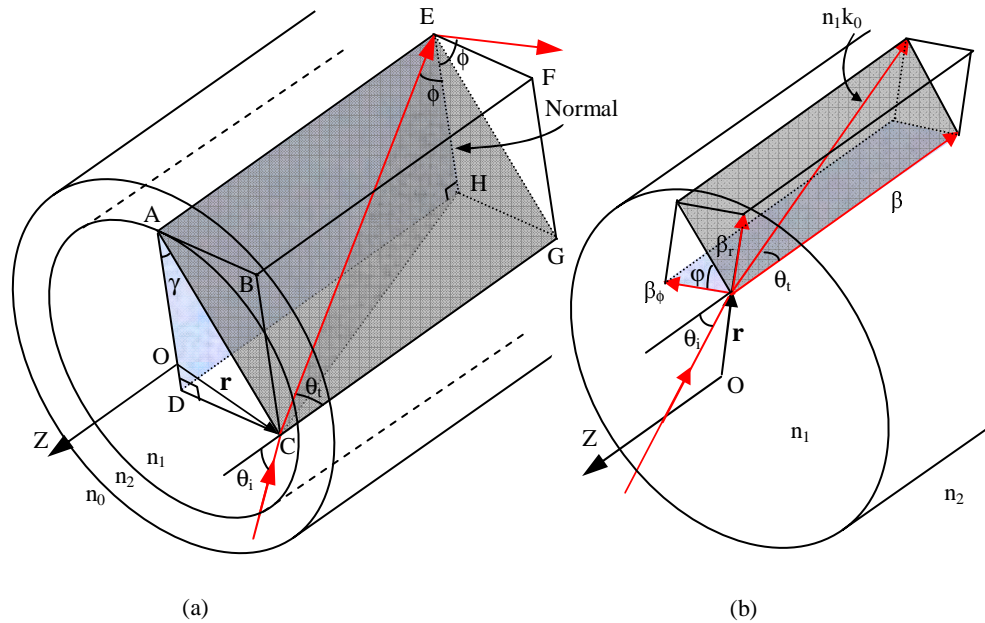


Fig. 2. Analysis of a skew ray under TIR and a tunnelling ray with associated mode just below cutoff. (a) Analysis of a skew ray formation at the position \mathbf{r} under TIR. (b) Local wave-vector decomposition for a ray incident on any position \mathbf{r} of a step-indexed fiber core end face.

As indicated before, there are fundamental differences between tunnelling rays and meridian / skew rays under TIR. Tunnelling rays do not follow the law of TIR. Instead, in terms of mode theory, the associated tunnelling modes belong to a group of leaky modes just below cutoff. Following the decomposition of the wave vector in Fig. 2(b), the propagation constant β of a leaky mode is limited by:

$$\sqrt{n_2^2 k_0^2 - \beta_r^2 - \beta_\phi^2} \leq \beta < n_2 k_0 \quad (11)$$

For a tunnelling mode, the radial component β_r must be real within the core, forming trapped power, imaginary in the cladding side adjacent to the core-cladding surface, forming an EW field, and again real beyond this EW layer, forming radiated power. By manipulating the wave vector components in the form of curves covering the core and cladding areas [26], Eq. (11) leads to a strict limit on the azimuthal component β_ϕ :

$$\beta_\phi = \frac{\nu}{\rho} \quad (12)$$

where ρ is the fiber core radius and ν is the azimuthal wave number. For a tunnelling mode, Eq. (11) thus becomes [26]:

$$\sqrt{n_2^2 k_0^2 - \frac{\nu^2}{\rho^2}} \leq \beta < n_2 k_0 \quad (13)$$

Similar to the procedure for deriving the acceptance angle of skew rays under TIR in Fig. 2(a), the acceptance angles of tunnelling modes have the following relationship [26]:

$$\sqrt{\frac{n_1^2 - n_2^2}{1 - (r/\rho)^2 \cos^2 \varphi}} \geq n_0 \sin \theta_i > \sqrt{n_1^2 - n_2^2} \quad (14)$$

or

$$\frac{NA_{mdn}}{\sqrt{1 - (r/\rho)^2 \cos^2 \varphi}} \geq n_0 \sin \theta_i > NA_{mdn} \quad (15)$$

Like a skew ray under TIR, a tunnelling ray, which is also skew, is formed by an incident ray with the minimum incident angle starting from the maximum acceptance angle of meridian rays. Its maximum acceptance angle, however, has a limited value depending on the combination of incident point r and the azimuthal angle φ . In particular, the incident rays associated with skew rays under TIR cannot excite tunnelling rays since tunnelling rays do not follow the restriction of TIR. The incident ray angles for meridian or skew rays under TIR and tunnelling rays are different. The possible entering positions are across the entire end face of the fiber core. The possible launching angles for these rays can vary within a vast range of $0 \leq \theta_i < \pi/2$.

2.6 Simultaneous excitation of higher-order guiding modes and tunneling modes, and suppression of lower-order guiding modes

The preceding analysis indicates that both enhancement of excitation power in the EW layer and the level of tunneled-back signal rely heavily on two mode groups: high-order modes as well as tunneling modes, with tunneling modes playing a more important role, especially for short fibers such as commonly found in fiber-optic sensor systems. Further optimization has to include the suppression of power in lower-order guiding modes. It is clear that such a power-coupling process is exactly the opposite of what is required in a fiber-optic communication system, where reduction of mode dispersion is the major concern and is ensured by solely boosting the lower-order guiding mode group.

The reason for requiring a source capable of achieving simultaneous excitation of these two mode groups now becomes clear. The incident ray angles must obey the following conditions of:

(a) confining the incident ray angles within the range:

$$\sin^{-1} NA_{mdn} \leq \theta_i < \pi/2 \quad (16)$$

with $n_0 = 1$; and

(b) allowing the incident rays to hit different positions across the core entrance surface and to uniformly excite all the desired modes.

However, it is difficult to use commercially available light sources directly to achieve this goal since most of their output power distribution, as mentioned before, is suited to excitation of lower-order guiding mode groups. The emission pattern of most sources can be expressed by:

$$B(\theta) = B_0 \cos^n \theta \quad (17)$$

where $n \geq 1$, B_0 is the radiance along the normal to the radiating surface.

Typically, an LED has $n \approx 1$ and is commonly called a Lambertian or diffuse source, showing relatively wider and more uniform angular distribution. An LD, however, has $n > 100$ [25], delivering energy in a much narrower cone. Both, on the other hand, have their power concentrated mainly on the normal to the radiating surface. Obviously, direct coupling by a traditional means will favor lower order-mode groups.

Tilting the conventional light source indicated by Eq. (17) to feed the main power to the maximum acceptance angle of the fiber might help to achieve the goal. The major drawback of a conventional source is that the source surface is not in direct contact with the fiber core. Instead, another optical component such as a lens is inserted in between to enhance the coupling efficiency. Unfortunately, the limited NA of the lens blocks most of the rays capable of exciting the desired modes, indicating that improvement of coupling to these modes through tilting of the source will be limited. We can also expect that a collimated light beam tilted to the fiber axis will have a limited effect on desired mode coupling due to the same reason, but it will, however, contribute to the suppression of lower-order guiding modes.

The above analysis suggests that a source emitting light rays whose direction changes randomly with isotropic intensity distributed in each direction might help to achieve the goal. Additionally, the source should send the light as directly to the fiber core as possible without the assistance of any NA-limited devices. We demonstrate such a source and its remarkable effect on performance enhancement via our experiments in the next section.

3. Experimental demonstration

3.1 Fabrication of fiber-optic side-emitting light diffuser (FOSED)

We propose a fiber-optic side-emitting diffuser (FOSED) as a light source with characteristics close to the requirements described at the end of the last section. A short segment of jacket at the fiber tip of a 3 meter MMF with core / cladding / jacket size of 400 / 430 / 730 μm is removed with a copper wire stripper. The exposed cladding layer is only 15 μm thick, forming a thin and roughened layer surrounding the fiber core. Part of the light in the fiber core will penetrate into the cladding and radiate into the surrounding space. The roughened cladding, with many irregular local sites, maneuvers light rays in all directions. The side-emitting effect of such a diffuser is shown in Fig. 3(a). Obviously, the output profile from this uncladded fiber segment (i-fiber) is that of a non-Lambertian light diffuser, sending light rays randomly in all directions.

The light from an Argon laser is coupled to this fiber at the other end. To enhance the strength of the diffuser light, the laser is focused off the center of the i-fiber axis, forming a bright ring that can be seen when observing the far-field mode field pattern at the other end of the i-fiber. The intensity at the fiber exit is adjusted to 3 mW.

3.2 Description of experimental setup

The experimental setup is shown in Fig. 4. A 2 meter r-fiber of the same type as i-fiber is decladded in the middle section, forming a 10 cm sensing segment sealed inside a flow cell. The decladded segment is fully exposed to the Rhodamine 6G sample fluid diluted with water to 29 $\mu\text{g} / \text{ml}$. The FOSED at the end of the illuminating fiber (i-fiber) is on a rotation stage with angle markers. With the r-fiber on another translation stage, each time the relative angle between the two fibers is changed, the optimum levels of the signal and noise of stray light can be ensured by adjusting the translation stage. A light-duty linear variable filter (LVF) is placed in front of the spectrometer to block part of the stray excitation light. A USB 2000 Spectrometer from Ocean Optics, together with a computer, is used for signal monitoring, and for data acquisition and processing.

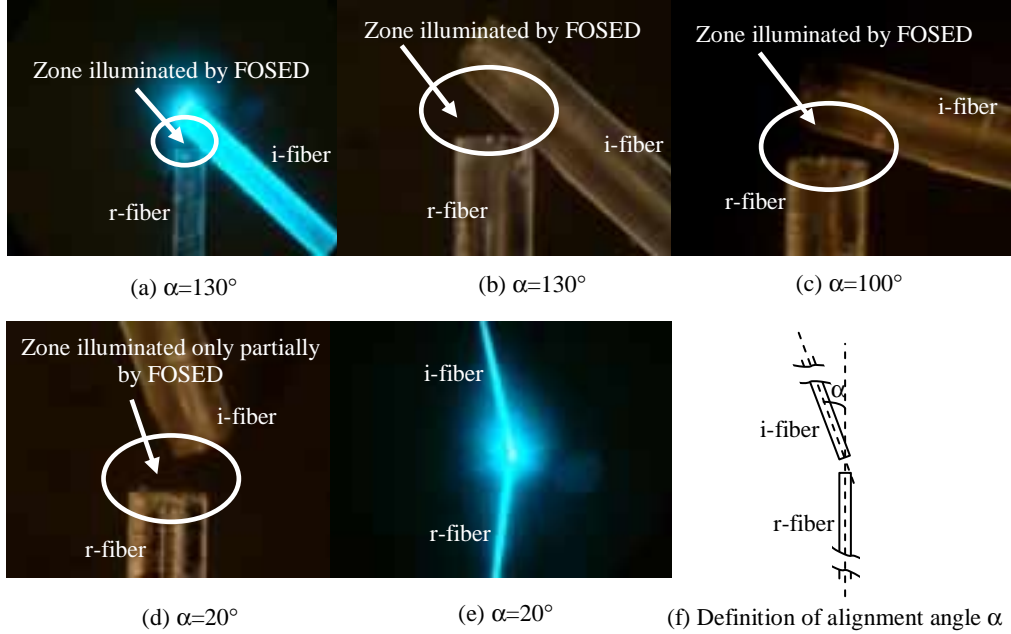


Fig. 3. Photos showing several typical fiber alignment angles used to illustrate experimental results in Fig. 5 (i-fiber: illuminating fiber; r-fiber: receiving fiber; FOSED: fiber-optic side-emitting diffuser).

3.3 Experimental results

In association with the optimum signal and stray light noise level, Fig. 3(a) ~ (d) shows photos reflecting several typical relative positions of the i- and r-fibers for the angles $\alpha = 20^\circ$, 100° and 130° , with α defined in Fig. 3(f).

Figure 5 illustrates the spectra associated with residual stray excitation light and fluorescent signal levels. As indicated before, even with the LVF, at the alignment angle $\alpha=20^\circ$, although the r-fiber receives much higher excitation power from the i-fiber, the fluorescent signal level, shown in Fig. 5(a), shows little difference from the cases of $\alpha = 100^\circ$ and 130° in Fig. 5(b). In particular, at $\alpha=20^\circ$, very strong excitation light is directly sent to the spectrometer over the lower-order guiding mode group, severely saturating the CCD pixels. Such a saturation effect widens the laser spectrum, increases the entire background noise level and reduces the normal signal-noise spectrum gap as well as adds a distorted tail on the fluorescent spectrum. The major reason for these phenomena is that the laser light is so strong that it is scattered among the optical and mechanical parts inside the spectrometer many times, sending significant amounts of power to other locations of the CCD array without

obeying the dispersion equation. More critically, Fig. 3(d) clearly demonstrates that most of the excitation light in fact is delivered to the i-fiber in the form of more Lambertian-like or worse, limiting its energy in a narrow cone rather than randomly diffused. Consequently, no matter how the separation is adjusted between the two fibers, only a small proportion of light rays will have their incident angles falling into the range defined in Eq. (16). To completely remove the stray excitation light, a high-performance filter is required.

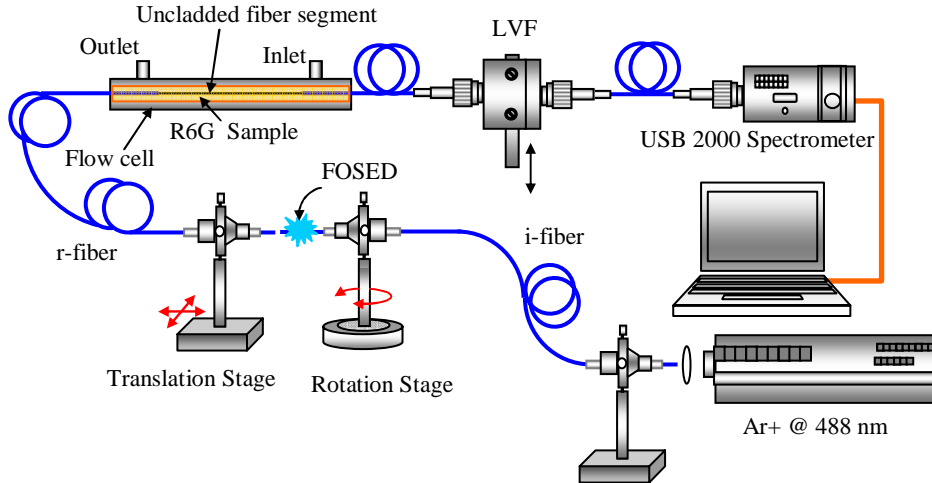


Fig. 4. Experimental setup (i-fiber: illuminating fiber; r-fiber: receiving fiber; LVF: linear variable filter).

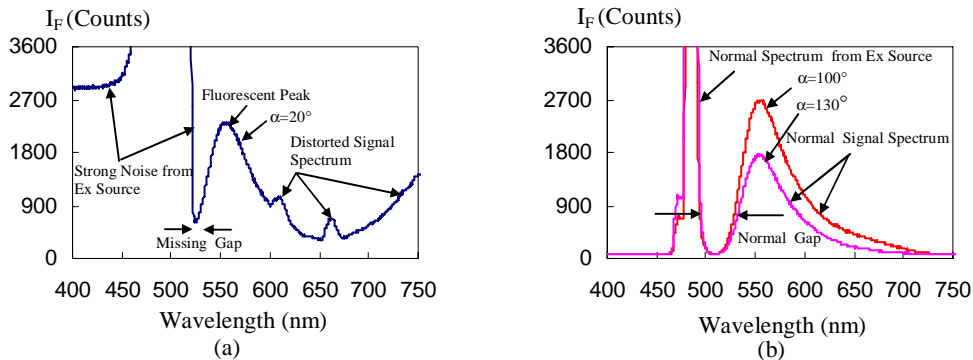


Fig. 5. Experimental curves associated with different fiber alignment angles. (a) Poor signal quality when the r-fiber is illuminated by the strong excitation power directly launched from the core of the i-fiber; (b) Dramatic improvement of signal quality when the r-fiber is illuminated by the FOSED.

On the other hand, at $\alpha=100^\circ$ or 130° , the r-fiber only receives diffused light from FOSED. Obviously, the overall power entering the r-fiber is much lower than is the case when $\alpha=20^\circ$. However, as illustrated in Fig. 5(b), the fluorescent signal quality is dramatically improved without sacrificing its level. Both the laser and signal spectra present normal profiles with a normal signal-noise spectrum gap and almost zero background level. Such a remarkable improvement suggests that a much larger proportion of randomly oriented light rays from the FOSED falls into the vast angle range defined by Eq. (16) and more higher-order guiding modes and tunnelling modes associated with different sites on the fiber core entrance surface are excited simultaneously. The fact that the FOSED evenly distributes light in all directions also ensures that much weaker power is spread into the lower-order guiding mode group. In other words, much lower excitation power will appear in the

receiving end, as evidenced again by the minimum spectra distortion in Fig. 5(b). The complete removal of the stray excitation light only demands a slightly enhanced performance of the filter, or can be simply set to zero via software programming.

4. Further discussion

Here we make a comparison between our EW MMF sensor and a long period grating (LPG) sensor since both involve mode coupling process.

An LPG written in a single-mode fiber core, under intensive research currently, has excellent core to cladding mode energy transfer capability. This is achieved by periodically changing the fiber properties such as the fiber core diameter or RI along the fiber. With sufficient mode field overlapping between core and cladding modes, an LPG forces a highly efficient core to cladding mode energy transfer within the length of the LPG, which may be in the order of approximately 1 ~ 2 centimeters.

Mode coupling in an MMF, however, is a slow process because of the lack of such a periodical varying characteristic. The mode coupling in an MMF is mainly due to the fiber defects such as the random change of the fiber size and the material properties. Once the light starts to propagate along the fiber, the energy transfer from the lower-order guiding mode group to the higher-order guiding one holding longer EW tails in the cladding side can be in general ignored. This is particularly the case when fiber is short. An intuitive consideration is that we may launch the excitation light directly into the fiber core to excite the core modes first and rely on the LPG to complete the transfer of the energy to the cladding area for sample excitation.

However, it is too early to say an LPG fiber-optic sensor is superior to an MMF counterpart. The first barrier is the tiny core of the single mode fiber. Almost all LPGs under research today are built in single mode fibers. It is no doubt that without taking some expensive measures, compared with an MMF, huge amount of excitation light will be blocked. The second barrier is that the LPG is a band filter and the core to cladding mode coupling occurs only to the limited and isolated resonant bands. The excitation light source for fluorescence sample assays varies from a wide band halogen lamp, an LED or a laser with extremely narrow band. The sample under investigation usually allows a wide spectrum of excitation light. Matching the LPG resonant bands to the specific sample excitation wavelength band requirement is obviously not an easy process. The third barrier is that even if such a matched band or bands are established, they suffer fluctuations due to other factors such as temperature or strain variations. This will in turn cause the undesired fluctuations of both the excitation power and the fluorescent signal levels. The fourth barrier is that once the sample is changed, this LPG may possibly become useless since the excitation band or bands are likely to be different. The fifth barrier concerns the coupling efficiency from the cladding modes to the core mode(s), which is needed for fluorescent signal collection. Most of the fluorescent signal is carried by huge number of cladding modes. But only one or few core modes (if the light wavelength is under cutoff) are allowed in a single mode fiber. How much signal power will be coupled back from these cladding modes to the core mode(s) is questionable. The enormous number of higher-order guiding and tunneling modes in an MMF obviously wins out in this competition.

Based on the analysis above, the advantages of our innovation are obvious. The non-Lambertian light diffuser will excite the higher-order guiding and tunneling modes simultaneously from the MMF end face. This direct excitation process from outside circumvents the use of the weak mode coupling from lower to higher order modes to boost the EW power level. By additionally considering the low-cost components and their alignments in the system, the proposed EW fiber-optic fluorometer is superior to the existing LPG fiber-optic sensor design.

5. Conclusion

In conclusion, we have proved, both theoretically and experimentally, that the higher-order guiding modes and tunneling modes, associated with steeper meridian and skew rays near the

critical angle and with tunneling rays, are the major factors affecting the performance of an EW-based MMF fluorometer. Under TIR, far more skew rays than meridian rays are capable of enhancing EW power and fluorescent signal levels. The tunneling mode group, with its mode population comparable to that of overall guiding modes and with its EW and radiating fields extending into the cladding much further, plays a critical role in the system performance, particularly when a large mode volume and a short length of fiber are involved.

The experimental results confirm that a poor signal quality can be expected when directly adopting a traditional light source and coupling means used in fiber-optic communication or fiber-optic sensor systems. Although the proposed FOSED has very low coupling efficiency, the signal quality is greatly enhanced without signal level penalty, suggesting the great potential of this non-Lambertian FOSED.

Our investigation shows that the negative factors or approaches from the point of view of a fiber-optic communication system or other optical systems can play positive roles in designing a fiber-optic sensor system. These include: 1. deliberately exciting the higher-order guiding and the tunneling modes but suppressing the lower-order guiding ones; 2. using a non-Lambertian light diffuser as a light source; 3. changing the way of light coupling, which goes against the conventional approach. These innovations together deliver the excitation light power in a more efficient way and lead to numerous benefits: lower demand on light source power level, lower demand on strict light coupling, lower demand on filter and detection system and finally, a high performance system with low cost.

Acknowledgements

The authors gratefully acknowledge support for this project from the Natural Sciences and Engineering Research Council of Canada and from the Canada Research Chairs Program.